Air Stagnations for China (1985–2014): Climatological Mean Features and Trends

Qianqian Huang, Xuhui Cai, Yu Song, Tong Zhu

College of Environmental Sciences and Engineering, State Key Joint Laboratory of Environmental Simulation and Pollution Control, Peking University, Beijing, 100871, China

Correspondence to: Xuhui Cai (xhcai@pku.edu.cn)

Abstract. Air stagnation is an important meteorological measurement for unfavourable air pollution conditions, but little is known about it in China. We conducted a comprehensive investigation of air stagnation in China, based on sounding and surface observations of 81 stations, from January 1985 to December 2014. The stagnation criteria were revised to be topographically dependent for the great physical diversity in this country. It is found that the annual mean air stagnation occurrences are closely related to general topography and climate features. Two basins in the northwest and southwest of China—Tarim and Sichuan Basins—exhibit the most frequent stagnation occurrence (50% days per year), whereas two plateaus (Tibet-Qinghai and Inner Mongolia Plateau) and the east coastal areas experience the least (20% days per year). Over the whole country, air stagnations achieve maxima in summer and minima in winter, except for Urumqi, a major city in the northwest of China, where stagnations keep a rather constant value yearly around with a minimum in spring. There is a nationwide positive trend in stagnation occurrence during 1985–2014, with the strongest increasing centres over Shandong Peninsula in eastern China and the south of Shaanxi in central China. Dependence degrees of air stagnations on three components (upper- and lower-air winds, precipitation-free days) are examined. It shows that the behaviours of upper-air wind speeds are main drivers of the spatial distribution and trend of air stagnations, near-surface winds the next, and dry days contribute the least.

1 Introduction

Air quality is strongly dependent on meteorological state, which controls the transport and dispersion of air pollutants within the lower atmosphere. The meteorological state with lingering anticyclones and persistent calm winds leading to poor ventilation and no precipitation to wash out pollutants is defined as an air stagnation event

(Wang and Angell, 1999). It has been observed that stagnation events are usually related to air pollution episodes (Jacob et al., 1993; Wang and Angell, 1999; Mickley et al., 2004; Wu et al., 2008; Fiore et al., 2012). For example, ozone measurements from rural sites in the eastern and western United States in 1978 and 1979 indicated that the majority of ozone episodes occurred during air stagnant conditions (Logan, 1989). The stagnation of air masses led

5 to an enhancement of surface ozone and CO mixing ratios over Western/Central Europe (Ordóñez et al., 2010; Leibensperger et al., 2008), and a 2.6 μg m^{-3} increase of fine particulate matter in the United States (Tai et al., 2010). The sensitivity of air quality to stagnations has been investigated by perturbing meteorological variables in regional chemical transport models (Liao et al., 2006). Jacob and Winner (2009) collected and compared results from different perturbation studies about the effects of weather conditions on ozone and particulate matter

10 concentrations, and summarized that air stagnation demonstrates a robust positive correlation. However, actual air pollution level is affected by not only meteorological conditions, but also other complex factors such as emission sources and chemical reactions (Cao et al., 2007; Guo et al., 2009; He et al., 2011; Yang et al, 2016). With other factors unknown, the air stagnation index may show poor correlation to actual air pollution data, in certain situations. The strength of air stagnation index is that, it provide an independent view to the meteorological

15 background relevant to air pollution, without being interfered by the complexity of other factors such as the variation of source emissions (Horton et al., 2014).

Air stagnation is identified by thresholds of daily upper- and lower-air winds and precipitation (Wang and Angell, 1999). The "upper-air winds" here refer to winds at about 5 km above the ground. From a meteorological

20 perspective, this level is important because of its connection to near-surface synoptic systems. It is found that the movement of surface cyclones tend to travel in the direction of the upper flow at roughly a quarter to half of the speed (Frederick et al., 2012). These kinds of near-surface synoptic systems are essential to air pollution (Jacob and Winner, 2009; Cai et al., 2017). On the other hand, near-surface winds and precipitation determine dilution and washout of air pollutants, both of them are also relevant to practical air quality. Therefore, the air stagnation

25 is a relatively simple, but conceptually robust metric to air pollution.

In previous works by Korshover (1967) and Korshover and Angell (1982) for the United States, air stagnation events were defined using daily weather maps from the US National Weather Service. They are periods with (i) the surface geostrophic wind is less than 8 m s^{-1}, generally corresponding to a 10m wind speed less than 3.2 m s^{-1}

30 (Wang and Angell, 1999); (ii) the wind speed at 500 hPa is less than 13 m s^{-1}; (iii) no precipitation. Wang and

Angell (1999) followed this metric but replaced the dataset with US National Centres for Environment Prediction (NCEP)/National Centre for Atmospheric Research (NCAR) reanalysis archive (2.5 °× 2.5 °). With this dataset, they studied the climatology of air stagnation for the United States from 1948 to 1998 and found that air stagnation events happen most frequently in the southern states during an extended summer season from May to October. Based on the work of Wang and Angell (1999), the National Climatic Data Center (NCDC) monitors air stagnation days in the United States with a finer gridded reanalysis data (0.25 °× 0.25 °) and provides maps about air stagnation distribution every month (http://www.ncdc.noaa.gov/societal-impacts/air-stagnation/). Following the NCDC's metric, Leung and Gustafson (2005) examined the potential effects of climate change on U.S. air quality by analyzing the simulated changes in stagnation events during 2045–2055. Horton et al. (2012, 2014) furthered this work and used a multi-model ensemble to project the future air stagnation occurrence on a global scale. They found that global warming could be expected to result in increasing stagnation frequency over the eastern United States, Mediterranean Europe and eastern China.

China has experienced rapid economic growth and industrialization in the recent decades and become the second largest energy consumer in the world (Chan and Yao, 2008). Tremendous energy consumption results in heavy air pollution. Research on its air quality is indispensable and studies of the relevant meteorological states are essential. Up to now, to the authors' knowledge, studies about air stagnation generally focused on the United States or on a global scale. Our focus in the current study is investigating the climatological mean features and trends of air stagnations for China, based on 30-year (1985–2014) observations on stations across the country.

2 Data and Method

2.1 Data

Long-term (1985–2014) dataset of daily-mean surface wind speeds (observed at 10 m above the surface) and daily precipitation data were obtained from China Meteorological Administration (CMA). These data are available at website (http://data.cma.cn/data/detail/dataCode/SURF_CLI_CHN_MUL_DAY_CES_V3.0.html). Upper-air wind speeds were obtained from Wyoming University soundings database (http://weather.uwyo.edu/upperair/sounding.html). This database provides twice daily (0000 and 1200 UTC) atmospheric soundings from stations that participate in global data exchange. Daily averages of upper-air wind speed at mandatory levels of 500, 400, and 300 hPa were used here.

We obtained datasets of all the radiosonde stations across China (95 stations) and two stations (Blagovescensk and Vladivostok) outside but near the border of the country. Among them, 66 stations have corresponding surface datasets from CMA (See Appendix A). For each of the other 31 radiosonde stations, we considered the average of surface stations within 150 km as a substitute. In this way, we got additional 15 stations (See Appendix B). Air stagnations of these 81 stations are analyzed in this study. Figure 1 displays the distribution of the stations. It shows that there are relatively less stations in Tibet-Qinghai Plateau, particularly in the western Tibet. Besides of this, the 81 stations cover all the contiguous China well.

2.1.1 Quality Control

Surface datasets have been quality controlled by CMA (http://data.cma.cn/data/detail/dataCode/SURF_CLI_ CHN_MUL_DAY_CES_V3.0.html). Upper-air winds data were eliminated from this analysis if

$$\left| U_i - \bar{U} \right| > 2\sigma , \tag{1}$$

where U_i denotes the i th upper-air wind speed at a given mandatory pressure level of a certain station, i ranges from 3 to $n\text{-}2$ and n is the total number of the data sample. $\bar{U}$ and σ are calculated as follows:

$$\bar{U} = \frac{1}{5} \sum_{i=i-2}^{i+2} U_i , \tag{2}$$

$$\sigma = \sqrt{\frac{\sum_{i=i-2}^{i+2} \left(U_i - \bar{U} \right)^2}{4}} , \tag{3}$$

Subjective quality control procedure was also applied. Time series plot of upper-air wind speeds at each station was drawn to screen temporally inhomogeneous data. Under these two quality control procedures, no upper-air wind data have been considered abnormal and removed. Therefore, we consider the data used in this study are reliable.

2.1.2 Data Completeness

A general survey shows that datasets of 73 stations are available from January 1985 to December 2014, while the other 8 stations (Wenjiang, Jinghe, Chongqing, Shanghai, Vladivostok, Yuzhong, Zhangqiu, Qingyuan) cover less than 30 years. The shortest duration is 7 years and 3 months (200710–201412) at Jinghe station. The percentage of valid data (data of upper- and lower-air wind and precipitation all valid) of each station is

summarized in Appendices A and B. It is shown that for all stations except Blagovescensk, more than 95% of the data are valid. Overall, the datasets are sufficient to conduct a climatological research about air stagnations over China.

2.2 Method

5   We adjust the NCDC air stagnation index and a given day is considered stagnant when daily total precipitation is < 1 mm (i.e. a dry day), daily-mean surface wind speed is < 3.2 m s^{-1} and upper-air wind speed is < 13 m s^{-1}. In previous studies, the upper-air wind is defined as the wind at 500 hPa. For China, however, this criterion is not appropriate for its great physical diversity. Particularly, the Tibet-Qinghai Plateau has the average height of over 4000 m. The wind speeds at 500 hPa are not a good representative to the upper-air winds above ground.

10   Therefore, we refined the criteria to be topographically dependent and the mandatory level to provide upper-air wind is chosen according to the station's elevation (Table 1).

With the modified criteria, air stagnation days are identified by checking meteorological conditions of every day at each station. Furthermore, if there are 4 or more consecutive days of air stagnation conditions at a given station,

15   those days are considered as one air stagnation case (Wang and Angell, 1999). Results of stagnation days and cases were interpolated with cubic splines to $2°\times 2°$ grid to show the spatial distribution over continental China.

3 Results

3.1 Annual Occurrence

Annual mean air stagnation days are distributed with substantial regional heterogeneity (Fig. 2a). They are most

20   prevalent over basins in the northwest and southwest of China (i.e., Xinjiang and Sichuan provinces) where air stagnant conditions account for 50% of days per year on average, and less prevalent (about 33% days per year) over the northernmost and southernmost of the country. The remainder domains of China experience even less stagnant days, especially Tibet-Qinghai Plateau, Inner Mongolia Plateau and the east coastal areas, where stagnant conditions are the least (less than 20% days per year). The distribution of stagnation cases agrees well

25   with that of stagnation days (Fig. 2b). The strongest stagnant centers—Xinjiang and Sichuan basins—exhibit more than 16 cases per year, while the weakest centers—Tibet-Qinghai and Inner Mongolia Plateau and east coastal areas—only experience less than 2 cases per year. Air stagnation cases usually persist about 5 days in a

majority of these areas (Fig. 2c). The ones over basins of Xinjiang and the southern China last longer (6 days). The longest duration of air stagnation conditions occurs in the south of Guangxi, lasting more than 7 days.

3.2 Seasonal Occurrence

Generally, most air stagnant conditions happen during summer season while only a few of those occur during winter. Stagnation days in autumn are slightly more than those in spring (Fig. 3). Similar feature was also found in the earlier work of Wang and Angell (1999) for the United States. The seasonal variation of stagnation is attributed to seasonal shift of pressure patterns and general circulation. A much weaker pressure gradient in summer is a well-known seasonal feature in mid-latitudes (Frederick et al., 2012). This feature is very evident in upper layer atmosphere in China (Ding et al., 2013, their Fig. 1.1). However at sea-level surface, the case in eastern Asia and China are complicated by the sub-tropical high in the east and the continental low and in the west respectively. As a result, Asia summer monsoon prevails in eastern China. Though for this, the sea level pressure gradient in summer is still much weaker than that in winter (Ding et al., 2013, their Fig. 1.1). A weaker wind in both upper and surface layer accompanies the weaker pressure gradient, and results in more air stagnant occurrence in China and North America (Wang and Angell 1999).

We choose four stations (Harbin, Urumqi, Beijing and Chongqing shown in Fig. 1 as triangles) as well as the average of entire China (all stations in this study) to demonstrate the seasonal variation of air stagnation days and cases. Figure 4 shows that for all but Urumqi, stagnation days and cases begin to increase in March or May, then grow dramatically and achieve maxima in July or August, then fall sharply and reach minima in December or January. However, monthly stagnation days and cases of Urumqi show much small variation in a year with their minima in April. This may attributes to the unique local climate there. Xinjiang basin is isolated at the center of the continent, far away from the coast, and blocked by the huge Tibet-Qinghai Plateau in the south. Therefore, the East Asia monsoon, particularly the East Asia summer monsoon, which is prevailing in east of China, influences little to Xinjiang. As a result, the seasonal feature of the stagnation in Urumqi is different from that in east of China. By comparing between these stations, we find that stagnations over Chongqing, Beijing and Urumqi are more than the average level of the entire country. Among them, Chongqing station has the largest variation of stagnations, and Beijing the next. Urumqi keeps a relatively high stagnation frequencies throughout the year.

3.3 Trend of Stagnations

The majority of China exhibits positive trends about 10–20 days and 1–3 cases per decade in stagnation days and cases, respectively (Fig. 5a, b). The strongest center located in Shandong Province and the south of Shaanxi, with rising rates of more than 20 days and 3 cases per decade. Only four fragments exhibit weak decrease: the extreme north of China, regions located in the south of Gansu and north of Sichuan, the westernmost and the southernmost part of China. The negative trend of stagnation varies from 0 to 10 days and 0 to 1 case per decade over the first three regions, and 30 days and 5 cases per decade over the last region. We have assessed the statistical significance of above results and 52% of stations have passed the 0.05 significance test. Not only stagnation frequencies show an increase over large areas, the duration of stagnation cases also exhibits a nationwide extension about 0.3 day decade^{-1} (Fig. 5c). Only a few scattered regions show a gradually shortened stagnation duration, including the extreme north of China, Yangtze River Delta, and the westernmost and southernmost region.

Stagnation trends of four stations (Harbin, Urumqi, Beijing and Chongqing) are also discussed specifically, as well as the average results of the entire country. Figure 6 shows that all four stations exhibit positive trends in air stagnation days, ranging from 3 to 14 days decade^{-1}, and the national-averaged increasing rate is about 6 days decade^{-1}. Moreover, the two stations experiencing more stagnant days (Urumqi and Chongqing) exhibit a slower rising rate about 5 and 3 days decade^{-1}, respectively, whereas the other two stations having relatively less stagnations (Harbin and Beijing) show a faster rate about 14 and 8 days decade^{-1}, respectively.

4 Discussions

Air stagnation is identified based on the thresholds of three components: the lower- and upper-air wind speeds and precipitation-free days. Analysis of each individual component is helpful in understanding the behaviour of stagnations. Figure 7a shows that the distribution of annual mean upper-air wind field is reversely correlated to that of stagnation occurrences. The upper-air wind is relatively weak in the northeast of China, Tarim Basin, Sichuan Basin and the southernmost of the country, which are exactly the same four regions exhibiting frequent stagnations. Different from the pattern of upper-air wind field, surface wind field exhibits a strong wind center (> 3 m s^{-1}) around the northeast of China, and a weak one (about 1.5 m s^{-1}) in Sichuan Basin (Fig.7b). Surface wind speed over the remainder of China is around 2 m s^{-1}. The distribution of dry days (daily total precipitation

< 1 mm) is largely related to the latitude. Figure 7c shows that generally dry days in the north is more than that in the south. But, specifically, the south of Xinjiang Province experiences maximum dry days of more than 350 days per year, while the south of Shaanxi Province shows the minimum about 200 days per year.

5 We further analyse the degrees of stagnation's dependence on every individual component (Fig. 8). It implies that 76% (R^2) of the spatial variation in stagnant days can be explained by the distribution of upper-air wind fields. The correlation even reaches as high as 82% in autumn (Fig. S1 in the Supplement). The surface wind field only accounts for 20% and the spatial distribution of dry days barely influences the stagnation variation. Figure 7 and 8 show that stagnation occurrences result from the cumulative responses of individual stagnation components, but
10 the distribution of upper-air wind speed exerts the dominant influence. The same feature was also suggested in the global research by Horton et al. (2012) in the area of China.

Similarly, we examine the relationship of stagnation trends with each component (Fig. 9) and find that the pattern of trends in upper-air wind field is similar to that of stagnant conditions. Decreases in upper-air wind field
15 substantially outnumber increases throughout the country (Fig. 9a), and the regions showing rapidly decreasing winds coincide with those exhibiting robust growing stagnations in Fig. 7. Trends in surface wind field and dry days may show a slightly different pattern from trends in stagnation (Fig. 9b, c), but they still contribute more or less for some regions. For areas with increasing stagnations like the northeast and the south of Shaanxi province, dry days show a substantial positive trend (about 3–7 days decade^{-1}) and upper- and lower-air wind speeds show
20 a remarkable negative trend (about 0.3–0.6 m s^{-1} decade^{-1}). For Shandong region, both upper- and lower-air wind speeds exhibit a substantial decrease of more than 0.3 m s^{-1} decade^{-1}, although the dry days show a slightly decrease about 1 day decade^{-1}. To summarize, the stagnation trends are contemporaneous effects of two or three components.

25 The dependence degrees of national averaged stagnation trends on every individual component are shown in Fig. 10. It can be seen that the negative trend in upper-air wind speed accounts for 73% of the increase in stagnant days. The ratio varies slightly with seasons and the highest one (79%) occurs in spring (Fig. S2 in the Supplement). Inter-annual variations in surface wind speed and dry days explain 42% and 32%, respectively. Still, trend in upper-air wind is the dominant contributor.

30

The trends of these three components (upper-air winds, near-surface winds and daily precipitation) are driven by climate change. The decrease in upper-air winds is resulted from smaller contrasts of the sea level pressure and a weakened Hadley circulation, both as a consequence of global warming (Lau et al., 2006; Lu et al., 2007; Seidel et al., 2008). Near-surface wind decline is attributed to the slowdown in atmospheric general circulation (Guo et al., 2011; Xu et al., 2006; Vautard et al., 2010) and stabilized atmosphere by light absorbing aerosols (Li et al., 2016; Peng et al., 2016; Wang et al., 2013). The decreasing number of rainy days is also closely related to the accumulation of greenhouse gases and anthropogenic aerosols (Gong et al., 2004; Liu et al., 2015; Wang et al., 2016). To sum up, climate changes alter atmospheric circulation and the hydrological cycle, which influence the occurrences of air stagnations—the meteorological background of air quality.

Stagnation is a meteorological metric for potential air pollution occurrence. Once there exist anthropogenic or natural air pollutants, they are liable to accumulate and result in poor air quality over regions that experience frequent air stagnant conditions. In contrast, over regions with infrequent stagnations, air pollutants will quickly be transported far away and diluted. Current results of the prevalent centers of stagnation days and cases are consistent with areas of heavy pollutions in China (Mamtimin and Meixner, 2007; Wang et al., 2011; Chen and Xie, 2012; Liu et al., 2013; Zhang et al., 2014; Li et al., 2015). It confirms that stagnation is an effective metric to measure the potential unfavourable meteorological states on air quality.

It should be noted that air stagnation metric does not take into account emissions or atmospheric chemical reactions. So there may be discrepancies between variations of stagnation index and actual air pollutant concentrations in certain situations. For example, aerosol concentration in China is characterized by high value in winter and lower one in summer. This observational fact is obviously related to the seasonal variation of source emission, since there is more coal consumption in winter for heating, particularly in north China (Cao et al., 2007; He et al., 2011). To make this kind of meteorological metric applicable for practical air pollution forecasting, Yang et al. (2016) incorporate source emission information into their PLAM index, and improve the forecasting skill successively. In this work, we aim to analyse the general features of meteorological background relevant to air pollution by means of the air stagnation metric, without concerning more about the complexity of source emissions or chemical reactions.

5 Conclusions

Based on upper and surface wind speeds and daily precipitation data from 81 stations across the country, this paper presented climatological mean values and trends of air stagnations for China, in the period from January 1985 to December 2014. The dependence of stagnations on three components (upper- and lower-air winds and dry days) was examined. A topographically dependent version of air stagnation criteria was applied to account for the terrain effect in China.

Annual mean of air stagnation occurrence varies spatially, in agreement with topography and climate features. Two basins in the northwest and southwest of China—Tarim and Sichuan Basins—exhibit the most frequent stagnation occurrence (50% days per year), while two plateaus (Tibet-Qinghai and Inner Mongolia Plateaus) and the east coastal areas experience the least (20% days per year). Seasonal variation of air stagnations is also presented. For a general view of the whole country, stagnations happen the most frequently in summer and the least in winter. For specific stations of Harbin, Beijing and Chongqing, stagnations vary with months dramatically and achieve maxima in July or August and minima in December or January, whereas stagnations in Urumqi keep a rather constant value with minimum in April.

There is a nationwide positive trend in stagnation days and cases, as well as case duration, in 1985–2014. The strongest increasing centres are located over Shandong Province in the eastern China and the south of Shaanxi in the central of the country. Only two exceptional regions—the southernmost and westernmost part of China—exhibit a negative trend in both occurrence and duration.

Stagnation occurrence contemporaneously response to three components, i.e., upper- and lower-air winds and precipitation-free days. Among them, upper-air wind speed plays a dominant role, explaining 76% and 73% of the spatial distribution and trend of air stagnations respectively. The lower-air wind exerts a minor influence. These results are corroborated by the global research from Horton et al. (2012). The spatial variation of dry days barely influences that of stagnations, whereas their inter-annual variability explains 32% of stagnation trend.

Air stagnation climatology presents a specific view to the natural background of atmosphere features being responsible to air pollution levels. The results presented in this paper may have significant implication to air pollution research, and may be used in atmospheric environment management or air pollution control.

Acknowledgements

This work is partially supported by National Natural Science Foundation of China (41421064, 41575007), Clean Air Research Project in China (Grant Nos. 201509001, 201409001), and National Key Technology Research and Development Program (2014BAC06B02). The authors would like to acknowledge CMA and Wyoming University for providing the long-term and public available surface observations and sounding data. The first author would like to thank Mr. Jian Wang for helping pre-process the sounding data. Two anonymous reviewers' comments and suggestions are greatly acknowledged.

Competing interests:

The authors declare that they have no conflict of interest.

Appendix A

The 66 radiosonde stations that have corresponding surface datasets from CMA. The periods for which radiosonde and surface datasets were both available are summarized with the start and end dates in the column date range. Data periods less than 30 years are highlighted in bold. The percentages of valid data are also presented here.

Station	ID*	Latitude (°N)	Longitude (°E)	Elevation (m)	Date Range	Valid Data
Hailar	50527	49.21	119.75	611	198501–201412	97.8%
Nenjiang	50557	49.16	125.23	243	198501–201412	98.9%
Harbin	50953	45.75	126.76	143	198501–201412	99.4%
Altay	51076	47.72	88.08	737	198501–201412	99.2%
Yining	51431	43.95	81.33	664	198501–201412	99.3%
Urumqi	51463	43.77	87.62	919	198501–201412	99.2%
Kuqa	51644	41.71	82.95	1100	198501–201412	99.4%
Kashi	51709	39.46	75.98	1291	198501–201412	99.2%
Ruoqiang	51777	39.02	88.16	889	198501–201412	99.1%
Hotan	51828	37.13	79.93	1375	198501–201412	99.4%
Hami	52203	42.81	93.51	739	198501–201412	99.3%
Dunhuang	52418	40.15	94.68	1140	198501–201412	99.1%
Jiuquan	52533	39.75	98.48	1478	198501–201412	98.9%
Minqin	52681	38.63	103.08	1367	198501–201412	98.5%
Golmud	52818	36.4	94.9	2809	198501–201412	99.2%
Dulan	52836	36.29	98.09	3192	198501–201412	96.9%
Xining	52866	36.71	101.75	2296	198501–201412	99.1%
Erenhot	53068	43.65	112	966	198501–201412	99.1%
Hohhot	53463	40.81	111.68	1065	198501–201412	99.3%
Yinchuan	53614	38.47	106.2	1112	198501–201412	98.2%
Taiyuan	53772	37.77	112.55	779	198501–201412	99.1%
YanAn	53845	36.59	109.5	959	198501–201412	99.3%
Pingliang	53915	35.54	106.66	1348	198501–201412	98.9%
XilinHot	54102	43.95	116.05	991	198501–201412	99.2%
Tongliao	54135	43.6	122.26	180	198501–201412	99.3%
Changchun	54161	43.9	125.21	238	198501–201412	99.0%

(Appendix A Continued)

Station	ID*	Latitude (°N)	Longitude (°E)	Elevation (m)	Date Range	Valid Data
Chifeng	54218	42.25	118.95	572	198501–201412	99.3%
Yanji	54292	42.88	129.46	178	198501–201412	99.4%
Shenyang	54342	41.75	123.43	43	198501–201412	99.2%
Linjiang	54374	41.71	126.91	333	198501–201412	98.9%
Beijing	54511	39.93	116.28	55	198501–201412	99.4%
Dalian	54662	38.9	121.62	97	198501–201412	99.3%
Lhasa	55591	29.65	91.12	3650	198501–201412	97.5%
Yushu	56029	33	97.01	3682	198501–201412	97.1%
Hezuo	56080	35	102.9	2910	198501–201412	98.4%
Garze	56146	31.61	100	522	198501–201412	98.7%
Wenjiang	56187	30.7	103.83	541	**200407–201412**	98.1%
Xichang	56571	27.9	102.26	1599	198501–201412	98.7%
Tengchong	56739	25.11	98.48	1649	198501–201412	99.1%
Kunming	56778	25.01	102.68	1892	198501–201412	99.0%
Simao	56964	22.76	100.98	1303	198501–201412	99.3%
Mengzi	56985	23.38	103.38	1302	198501–201412	99.2%
Zhengzhou	57083	34.7	113.65	111	198501–201412	99.3%
Hanzhong	57127	33.06	107.02	509	198501–201412	99.4%
Jinghe	57131	34.26	108.58	411	**200710–201412**	100.0%
Enshi	57447	30.28	109.46	458	198501–201412	99.4%
Yichang	57461	30.7	111.3	134	198501–201412	99.3%
Wuhan	57494	30.61	114.12	23	198501–201412	99.4%
Chongqing	57516	29.51	106.48	260	**198708–201412**	98.2%
Guiyang	57816	26.47	106.65	1222	198501–201412	98.0%
Guilin	57957	25.33	110.3	166	198501–201412	99.4%
Ganzhou	57993	25.85	114.94	125	198501–201412	99.1%
Xuzhou	58027	34.27	117.15	42	198501–201412	99.3%
Nanjing	58238	32	118.8	7	198501–201412	99.4%
Shanghai	58362	31.4	121.46	4	**199106–201412**	98.3%

(Appendix A Continued)

Station	ID*	Latitude (°N)	Longitude (°E)	Elevation (m)	Date Range	Valid Data
Anqing	58424	30.53	117.05	20	198501–201412	99.4%
Hangzhou	58457	30.22	120.16	43	198501–201412	99.3%
Nanchang	58606	28.6	115.91	50	198501–201412	99.1%
QuXian	58633	28.95	118.86	71	198501–201412	99.1%
Fuzhou	58847	26.07	119.27	85	198501–201412	99.3%
Xiamen	59134	24.47	118.08	139	198501–201412	99.3%
Baise	59211	23.9	106.6	175	198501–201412	99.2%
Wuzhou	59265	23.48	111.3	120	198501–201412	98.3%
Shantou	59316	23.35	116.66	3	198501–201412	99.2%
Nanning	59431	22.62	108.2	126	198501–201412	99.3%
Haikou	59758	20.03	110.34	24	198501–201412	99.2%

* World Meteorological Organization Identification Number.

Appendix B

Same as Appendix A, but for the 15 radiosonde stations and corresponding surface stations within 150 km.

Station	ID	Latitude (°N)	Longitude (°E)	Elevation (m)	Surface Stations (CMA)	Latitude (°N)	Longitude (°E)	Distance (km)	Date Range	Valid Data
Blagovescensk	31510	50.52	127.5	177	50353	51.43	126.4	127.58	198501–201412	65.9%
					50564	49.26	127.2	141.64		
Vladivostok	31977	43.26	132.05	82	54096	44.23	131.1	132.61	**199408–201412**	96.1%
					59287	23.1	113.2	132.7		
KingsPark	45004	22.3	114.16	66	59293	23.44	114.4	129.34	198501–201412	99.1%
					59501	22.48	115.2	110.8		
YuZhong	52983	35.87	104.15	1875	52884	36.21	103.6	65.18	**200107–201412**	94.5%
Linhe	53513	40.75	107.4	1041	53336	41.34	108.3	100.66	198501–201412	99.0%
					54725	37.3	117.3	70.05		
Zhangqiu	54727	36.7	117.55	123	54823	36.36	117	59.92	**200308–201412**	98.3%
					54843	36.45	119.1	142.05		
Qingdao	54857	36.06	120.33	77	54843	36.45	119.1	117.68	198501–201412	99.3%
Weining	56691	26.86	104.28	2236	57707	27.18	105.2	95.07	198501–201412	98.4%
					57265	32.23	111.4	141.85		
Nanyang	57178	33.03	112.58	131	57290	33	114	133.37	198501–201412	99.2%

(Appendix B continued)

Station	ID	Latitude (°N)	Longitude (°E)	Elevation (m)	Surface Stations (CMA)	Latitude (°N)	Longitude (°E)	Distance (km)	Date Range	Valid Data
Changsha	57679	28.2	113.08	46	57687	28.13	112.6	52.52	198501–201412	98.6%
Huaihua	57749	27.56	110	261	57745	27.27	109.4	66.58	198501–201412	99.2%
Sheyang	58150	33.75	120.25	7	58040	34.5	119.1	136.93	198501–201412	99.3%
					58251	32.52	120.2	136.88		
Fuyang	58203	32.86	115.73	33	58102	33.52	115.5	77.52	198501–201412	99.3%
					58221	32.57	117.2	143.98		
Shaowu	58725	27.32	117.45	219	58715	27.35	116.4	104.76	198501–201412	99.1%
					58834	26.39	118.1	121.86		
QingYuan	59280	23.66	113.05	19	59082	24.41	113.4	89.16	**199601–201412**	95.3%
					59287	23.1	113.2	64.13		
					59293	23.44	114.4	140.78		

References

Cai, W., Li, K., Liao, H., Wang, H., and Wu, L.: Weather conditions conducive to Beijing severe haze more frequent under climate change, Nat. Clim. Change, 7, 257–262, doi: 10.1038/nclimate3249, 2017.

Cao, J. J., Lee, S. C., Chow, J. C., Watson, J. G., Ho, K. F., Zhang, R. J., Jin, Z. D., Shen, Z. X., Chen, G. C., Kang, Y. M., Zou, S. C., Zhang, L. Z., Qi, S. H., Dai, M. H., Cheng, Y., and Hu, K.: Spatial and seasonal distributions of carbonaceous aerosols over China, J. Geophys. Res.-Atmos., 112, doi:10.1029/2006JD008205, 2007.

Chan, C.K. and Yao, X.: Air pollution in mega cities in China, Atmos. Environ., 42, 1–42, doi:10.1016/j.atmosenv.2007.09.003, 2008.

Chen, Y. and Xie, S.: Temporal and spatial visibility trends in the Sichuan Basin, China, 1973 to 2010, Atmos. Res., 112, 25–34, doi:10.1016/j.atmosres.2012.04.009, 2012.

Ding, Y. H., Wang, S. W., Zheng, J. Y., Wang, H. J., and Yang, X. Q.: Climate of China, Science Press, Beijing, 557pp, 2013 (in Chinese).

Fiore, A.M., Naik, V., Spracklen, D.V., Steiner, A., Unger, N., Prather, M., Bergmann, D., Cameron-Smith, P.J., Cionni, I., Collins, W.J., Dalsoren, S., Eyring, V., Folberth, G.A., Ginoux, P., Horowitz, L.W., Josse, B., Lamarque, J.F., MacKenzie, I.A., Nagashima, T., O'Connor, F.M., Righi, M., Rumbold, S.T., Shindell, D.T., Skeie, R.B., Sudo, K., Szopa, S., Takemura, T., and Zeng, G.: Global air quality and climate, Chem. Soc. Rev., 41, 6663–83, doi:10.1039/c2cs35095e, 2012.

Frederick, K. L., Edward, J. T., and Dennis, G. T.: The atmosphere: an introduction to meteorology, Prentice Hall, 528pp, 2012.

Gong, D. Y., Shi, P. J., and Wang, J. A.: Daily precipitation changes in the semi-arid region over northern China, J. Arid Environ., 59, 771-784, doi:10.1016/j.jaridenv.2004.02.006, 2004.

Guo, H., Xu, M., Hu, Q.: Changes in near-surface wind speed in China: 1969-2005, Int. J. Climatol., 31, 349-358, doi:10.1002/joc.2091, 2011.

Guo, J. P., Zhang, X. Y., Che, H. Z., Gong, S. L., An, X. Q., Cao, C. X., Guang, J., Zhang, H., Wang, Y. Q., Zhang, X. C., Xue, M., and Li, X. W.: Correlation between PM concentrations and aerosol optical depth in eastern China, Atmos. Environ., 43, 5876–5886, doi:10.1016/j.atmosenv.2009.08.026, 2009.

He, K. B., Yang, F. M., Ma, Y. L., Zhang, Q., Yao, X. H., Chan, C. K., Cadle, S., Chan, T., and Mulawa, P.: The characteristics of PM2.5 in Beijing, China, Atmos. Environ., 35, 4959–4970, doi:10.1016/S1352-2310(01)00301-6, 2001.

Horton, D.E. and Diffenbaugh, N.S.: Response of air stagnation frequency to anthropogenically enhanced radiative

forcing, Environ. Res. Lett., 7, 044034, doi:10.1088/1748-9326/7/4/044034, 2012.

Horton, D.E., Skinner, C.B., Singh, D., and Diffenbaugh, N.S.: Occurrence and persistence of future atmospheric stagnation events, Nature Climate Change, 4, 698–703, doi:10.1038/NCLIMATE2272, 2014.

Jacob, D.J., Logan, J.A., Gardner, G.M., Yevich, R.M., Spivakovsky, C.M., Wofsy, S.C., Sillman, S., and Prather, M.J.: Factors regulating ozone over the United States and its export to the global atmosphere, J. Geophys. Res.: Atmos., 98, 14817–14826, doi:10.1029/98JD01224, 1993.

Jacob, D.J., and Winner, D.A.: Effect of climate change on air quality. Atmos. Environ., 43, 51–63, doi:10.1016/j.atmosenv.2008.09.051, 2009.

Korshover, J.: Climatology of stagnating anticyclones east of the Rocky Mountains, 1936–1965 (Association of stagnating anticyclones with incidents of heavy air pollution in eastern United States from 1936 to 1965), 1967.

Korshover, J. and Angell, J.K.: A Review of Air-Stagnation Cases in the Eastern United States During 1981—Annual Summary, Mon. Wea. Rev., 110, 1515–1518, doi: 10.1175/1520-0493(1982)110<1515:AROASC>2.0.CO;2, 1982.

Lau, N. C., Leetmaa, A., and Nath, M. J.: Attribution of atmospheric variations in the 1997–2003 period to SST anomalies in the Pacific and Indian Ocean basins, J. Clim., 19, 3607-3628, doi:10.1175/JCLI3813.1, 2006.

Leibensperger, E.M., Mickley, L.J., and Jacob, D.J.: Sensitivity of US air quality to mid-latitude cyclone frequency and implications of 1980–2006 climate change, Atmos. Chem. Phys., 8, 7075–7086, doi:10.5194/acp-8-7075-2008, 2008.

Leung, L.R. and Gustafson, W.I.: Potential regional climate change and implications to US air quality, Geophys. Res. Lett., 32, 367–384, doi:10.1029/2005GL022911, 2005.

Li, X., Xia, X., Wang, L., Cai, R., Zhao, L., Feng, Z., Ren, Q., and Zhao, K.: The role of foehn in the formation of heavy air pollution events in Urumqi, China, J. Geophys. Res.: Atmos., 120, 5371–5384, doi:10.1002/2014JD022778, 2015.

Li, Z. Q., Lau, W. K. M., Ramanathan, V., Wu, G., Ding, Y., Manoj, M. G., Liu, J., Qian, Y., Li, J., Zhou, T., Fan, J., Rosenfeld, D., Ming, Y., Wang, Y., Huang, J., Wang, B., Xu, X., Lee, S. S., Cribb, M., Zhang, F., Yang, X., Zhao, C., Takemura, T., Wang, K., Xia, X., Yin, Y., Zhang, H., Guo, J., Zhai, P. M., Sugimoto, N., Babu, S. S., and Brasseur, G. P.: Aerosol and monsoon climate interactions over Asia, Rev. Geophys., 54, 866-929, doi:10.1002/2015rg000500, 2016.

Liao, H., Chen, W. T., and Seinfeld, J. H.: Role of climate change in global predictions of future tropospheric ozone and aerosols, J. Geophys. Res.-Atmos., 111, doi:10.1029/2005JD006852, 2006.

Liu, R., Liu, S. C., Cicerone, R. J., Shiu, C. J., Li, J., Wang, J. L., and Zhang, Y. H.: Trends of Extreme Precipitation in Eastern China and Their Possible Causes, Adv. Atmos. Sci., 32, 1027-1037, doi:10.1007/s00376-015-5002-1, 2015.

Liu, X.G., Li, J., Qu, Y., Han, T., Hou, L., Gu, J., Chen, C., Yang, Y., Liu, X., Yang, T., Zhang, Y., Tian, H., and Hu, M.: Formation and evolution mechanism of regional haze: a case study in the megacity Beijing, China, Atmos. Chem. Phys., 13, 4501–4514, doi:10.5194/acp-13-4501-2013, 2013.

Logan, J.A.: Ozone in rural areas of the United States, J. Geophys. Res.: Atmos., 94, 8511–8532, doi:10.1029/JD094iD06p08511, 1989.

Lu, J., Vecchi, G. A., and Reichler, T.: Expansion of the Hadley cell under global warming, Geophys. Res. Lett., 34, 5, doi:10.1029/2006gl028443, 2007.

Mamtimin, B. and Meixner, F.X.: The characteristics of air pollution in the semi-arid city of Urumqi (NW China) and its relation to climatological process, Geophys. Res. Abstr., 9, 06537, 2007.

Mickley, L.J., Jacob, D.J., Field, B.D., and Rind, D.: Effects of future climate change on regional air pollution episodes in the United States, Geophys. Res. Lett., 31, L24103, doi:10.1029/2004GL021216, 2004.

Ordonez, C., Elguindi, N., Stein, O., Huijnen, V., Flemming, J., Inness, A., Flentje, H., Katragkou, E., Moinat, P., Peuch, V.H., Segers, A., Thouret, V., Athier, G., van Weele, M., Zerefos, C.S., Cammas, J.P., and Schultz, M.G.: Global model simulations of air pollution during the 2003 European heat wave, Atmos. Chem. Phys., 10, 789–815, doi:10.5194/acp-10-789-2010, 2010.

Peng, J., Hu, M., Guo, S., Du, Z., Zheng, J., Shang, D., Zamora, M. L., Zeng, L., Shao, M., Wu, Y.-S., Zheng, J., Wang, Y., Glen, C. R., Collins, D. R., Molina, M. J., and Zhang, R.: Markedly enhanced absorption and direct radiative forcing of black carbon under polluted urban environments, Proc. Natl. Acad. Sci. U. S. A., 113, 4266-4271, doi:10.1073/pnas.1602310113, 2016.

Seidel, D. J., Fu, Q., Randel, W. J., and Reichler, T. J.: Widening of the tropical belt in a changing climate, Nat. Geosci., 1, 21-24, doi:10.1038/ngeo.2007.38, 2008.

Tai, A.P.K., Mickley, L.J., and Jacob, D.J.: Correlations between fine particulate matter ($PM_{2.5}$) and meteorological variables in the United States: Implications for the sensitivity of $PM_{2.5}$ to climate change, Atmos. Environ., 44, 3976–3984, doi:10.1016/j.atmosenv.2010.06.060, 2010.

Vautard, R., Cattiaux, J., Yiou, P., Thepaut, J.-N., and Ciais, P.: Northern Hemisphere atmospheric stilling partly attributed to an increase in surface roughness, Nat. Geosci., 3, 756-761, doi:10.1038/ngeo979, 2010.

Wang, J.X.L. and Angell, J.K.: Air stagnation climatology for the United States, NOAA/Air Resource Laboratory ATLAS, 1999.

Wang, Y., Khalizov, A., Levy, M., and Zhang, R. Y.: New Directions: Light absorbing aerosols and their atmospheric impacts, Atmos. Environ., 81, 713-715, doi:10.1016/j.atmosenv.2013.09.034, 2013.

Wang, Y., Ma, P.-L., Jiang, J. H., Su, H., and Rasch, P. J.: Toward reconciling the influence of atmospheric aerosols and greenhouse gases on light precipitation changes in Eastern China, J. Geophys. Res.-Atmos., 121, 5878-5887,

doi:10.1002/2016jd024845, 2016.

Wang, Y., Zhang, Y., Hao, J., and Luo, M.: Seasonal and spatial variability of surface ozone over China: Contributions from background and domestic pollution, Atmos. Chem. Phys., 11, 3511–3525, doi:10.5194/acp-11-3511-2011, 2011.

Wu S.L., Mickley L.J., Leibensperger E.M, Jacob, D.J., Rind, D., and Streets, D.G.: Effects of 2000–2050 global change on ozone air quality in the United States, J. Geophys. Res.: Atmos., 113, 304–12, doi:10.1029/2007JD008917, 2008.

Xu, M., Chang, C. P., Fu, C. B., Qi, Y., Robock, A., Robinson, D., and Zhang, H. M.: Steady decline of east Asian monsoon winds, 1969-2000: Evidence from direct ground measurements of wind speed, J. Geophys. Res.-Atmos., 111, doi:10.1029/2006jd007337, 2006.

Yang, Y. Q., Wang, J. Z., Gong, S. L., Zhang, X. Y., Wang, H., Wang, Y. Q., Wang, J., Li, D., and Guo, J. P.: PLAM–a meteorological pollution index for air quality and its applications in fog-haze forecasts in North China, Atmos. Chem. Phys., 16, 1353-1364, doi:10.5194/acp-16-1353-2016, 2016.

Zhang, J.K., Sun, Y., Liu, Z.R., Ji, D.S., Hu, B., Liu, Q., and Wang, Y.S.: Characterization of submicron aerosols during a month of serious pollution in beijing, 2013. Atmos. Chem. Phys., 14, 1431–1432, doi:10.5194/acp-14-2887-2014, 2014.

5 **Table 1. Station elevations and the corresponding upper-air wind speed criteria.**

Station Elevation (m)	Topographically dependent upper-air wind speed criterion
0–1000	wind speed at 500 hPa < 13 m s^{-1}
1000–3000	wind speed at 400 hPa < 13 m s^{-1}
3000–4000	wind speed at 300 hPa < 13 m s^{-1}
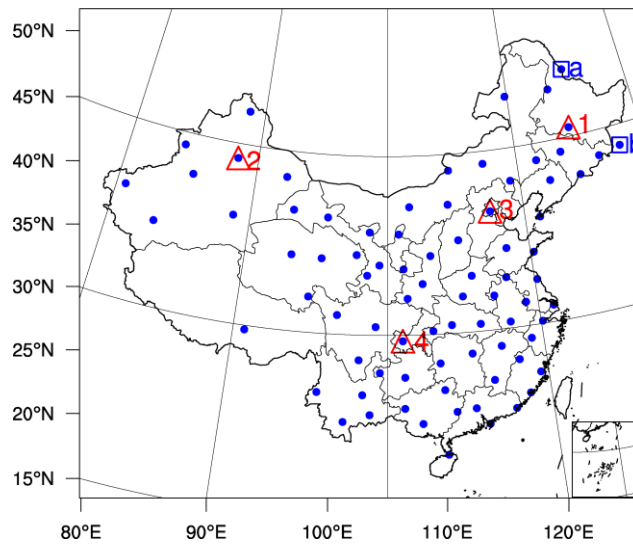
Figure 1. Distribution of observation stations. Triangles indicate four stations selected to discuss seasonal variations of air stagnations in Section 3: 1 for Harbin, 2 for Urumqi, 3 for Beijing, 4 for Chongqing. Squares indicate two stations outside of China: Blagovescensk (a) and Vladivostok (b).
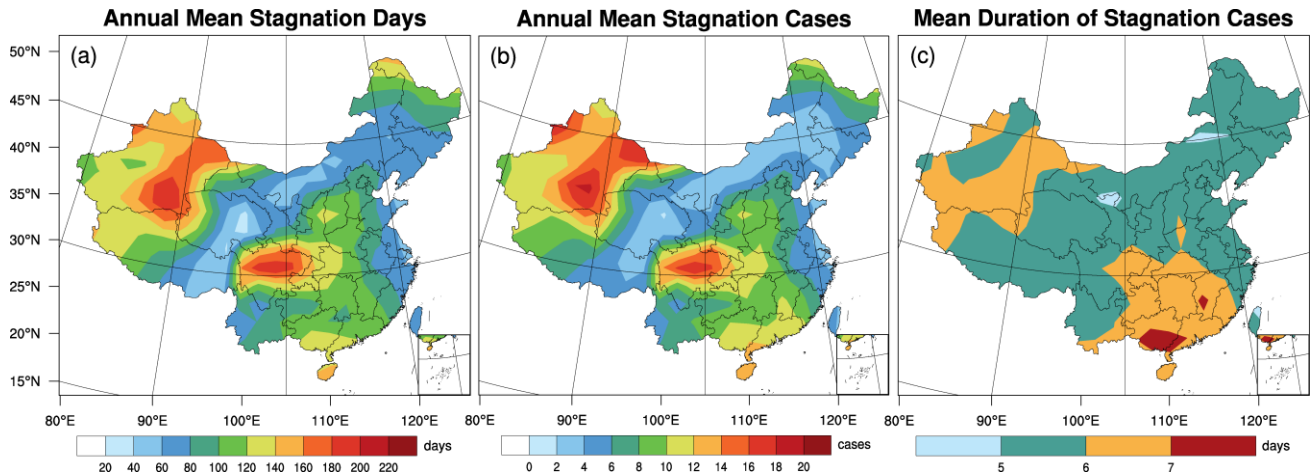
Figure 2. Annual mean air stagnation days (a) and cases (b) and mean duration of stagnation cases in days (c) for China (1985–2014).
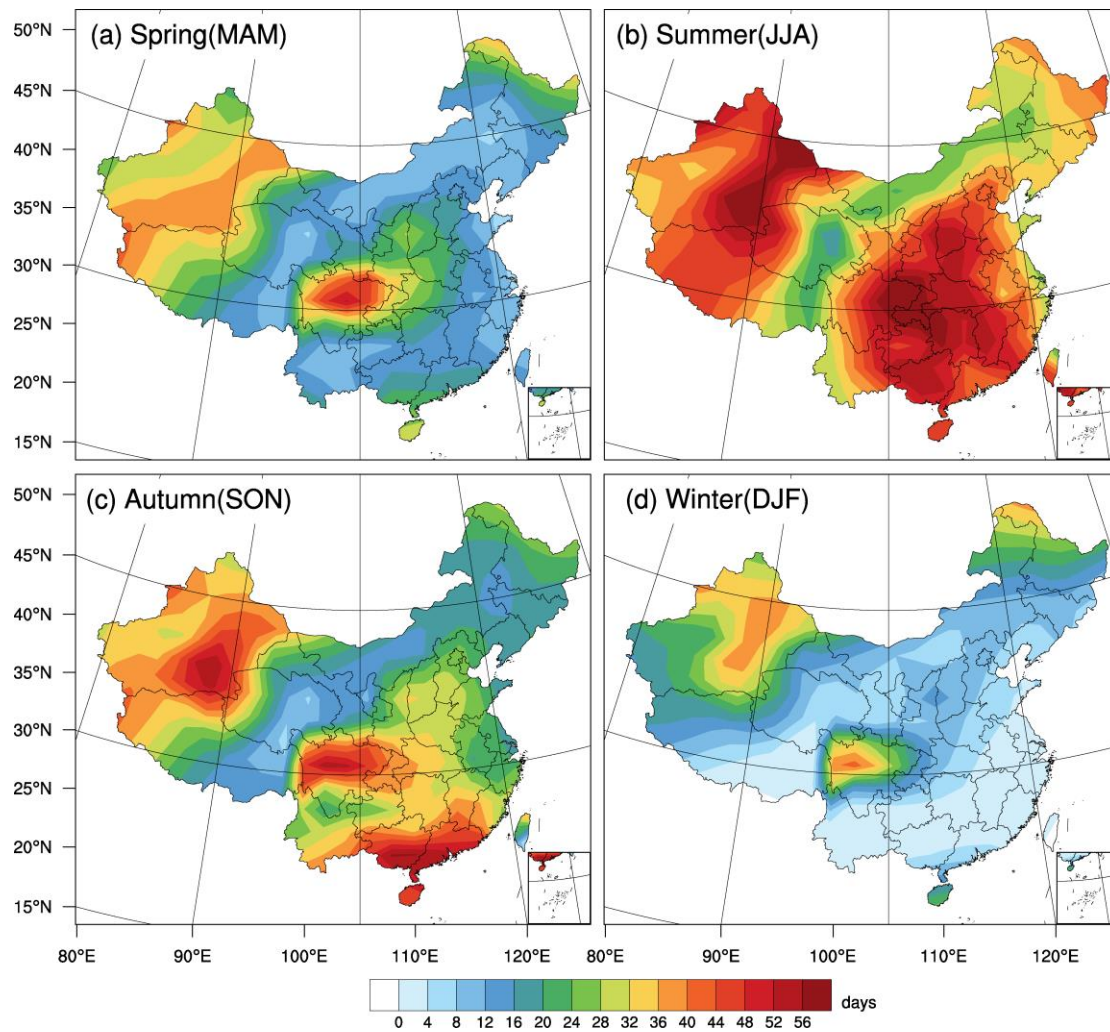
Figure 3. Average air stagnation days in spring (a), summer (b), autumn (c) and winter (d), 1985–2014.
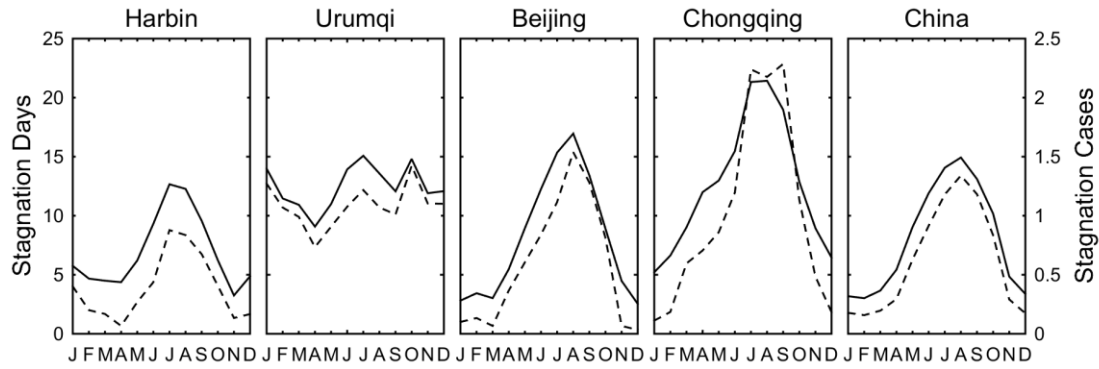
Figure 4. Seasonal cycles of monthly mean air stagnation days and cases for four stations (Harbin, Urumqi, Beijing and Chongqing) and the entire China. Solid line: stagnation days; dashed line: stagnation cases.
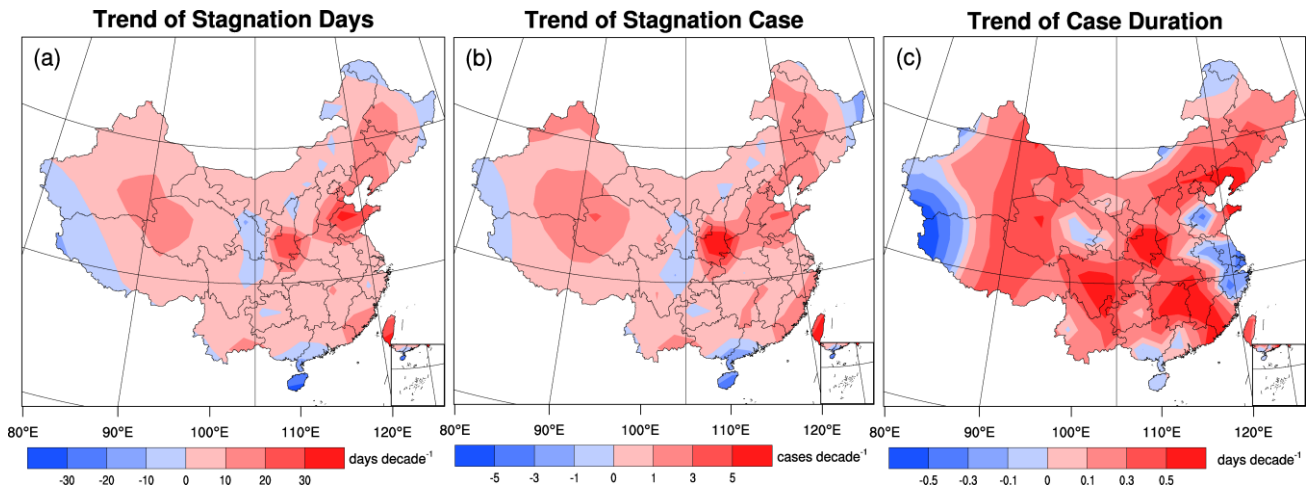
Figure 5. Trends of stagnation days (a), cases (b) and the duration of stagnation cases (c), 1985–2014.
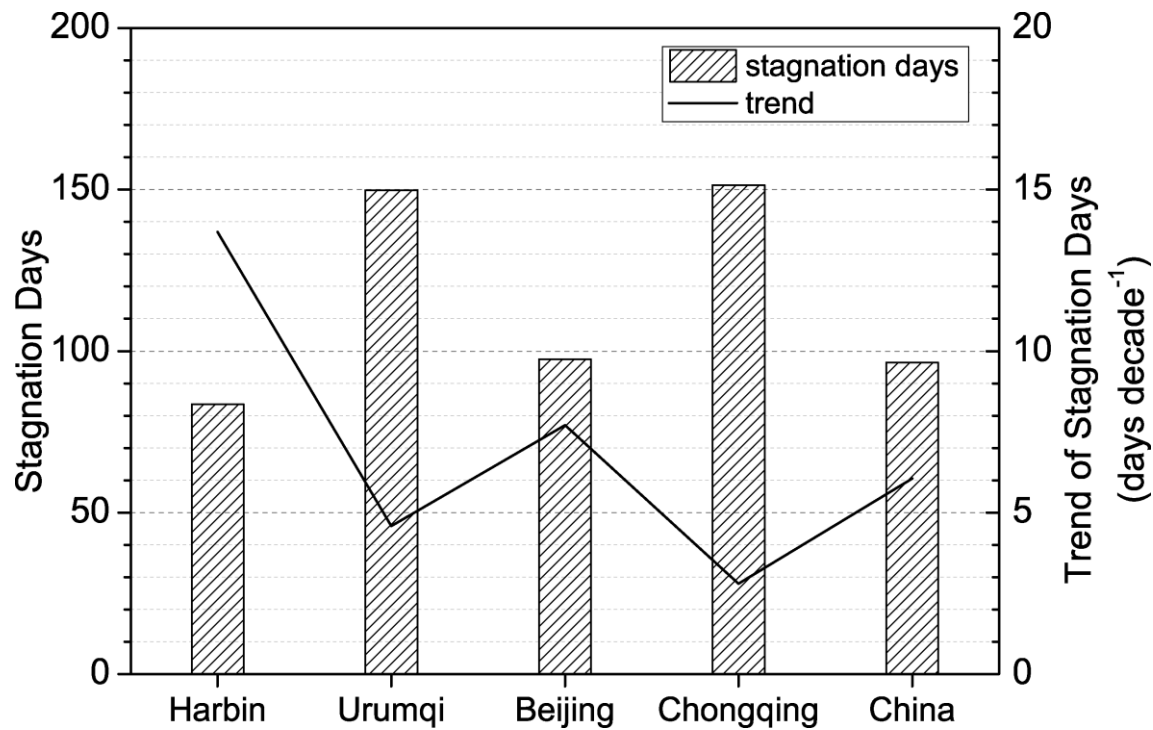
Figure 6. Annual mean stagnant days and the corresponding trend at four stations (Harbin, Urumqi, Beijing and Chongqing) and for the whole country.
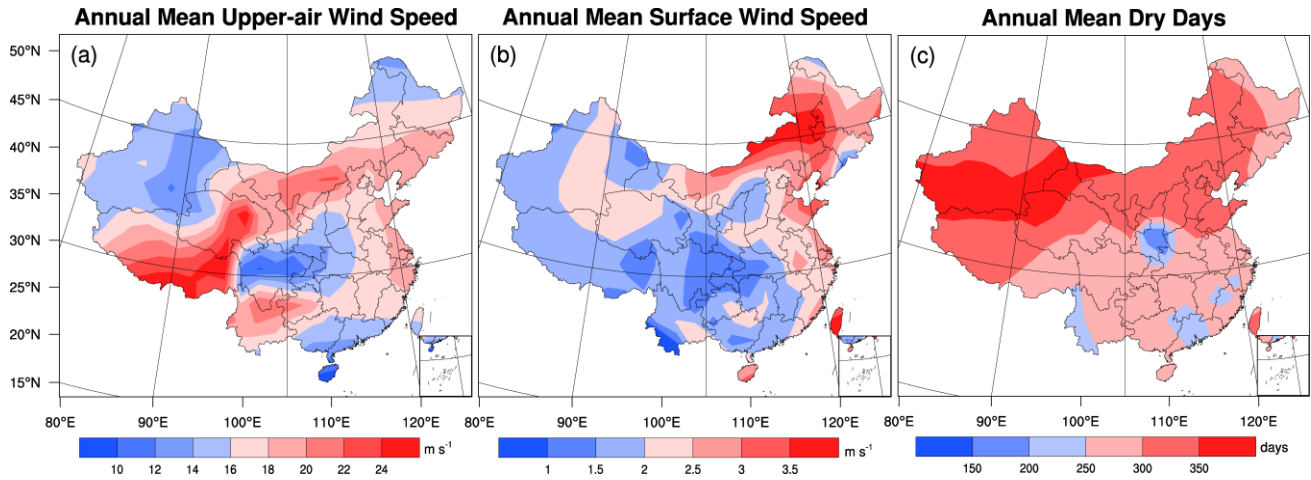
Figure 7. Annual mean upper-air wind speed (a), surface wind speed (b) and dry days (c) in China (1985–2014).
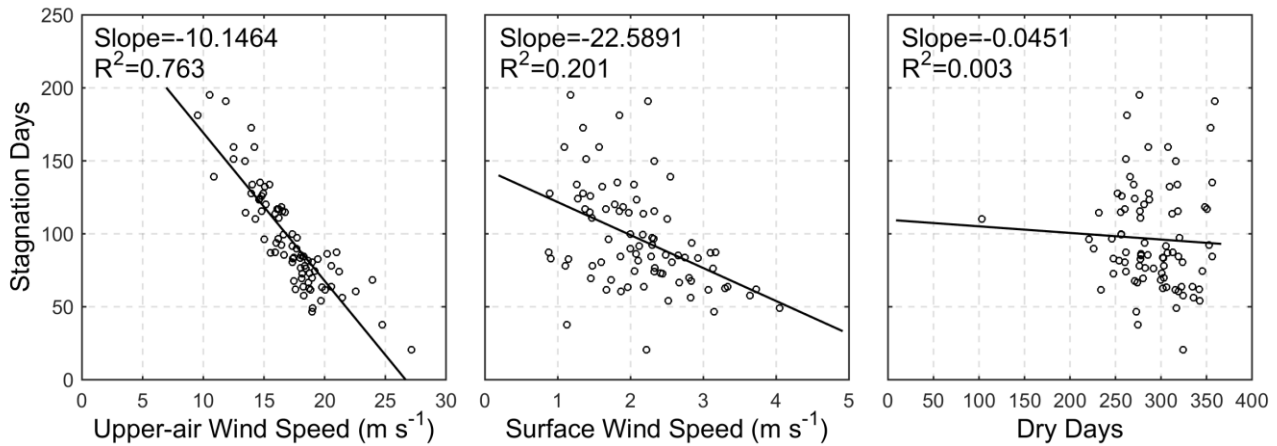
Figure 8. Dependence of spatial distribution of stagnation days on three components (upper-air wind speed, surface wind speed and dry days). Linear regression coefficients between annual mean stagnation days at 81 stations and each corresponding component are shown.
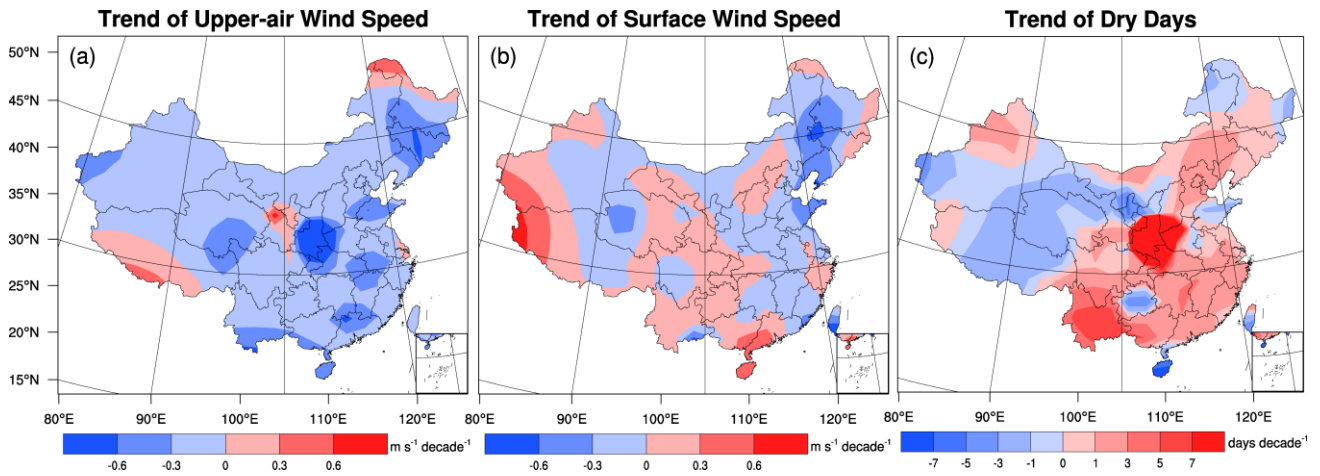
Figure 9. Trends of upper-air wind speed (a), surface wind speed (b) and dry days (c), 1985–2014.
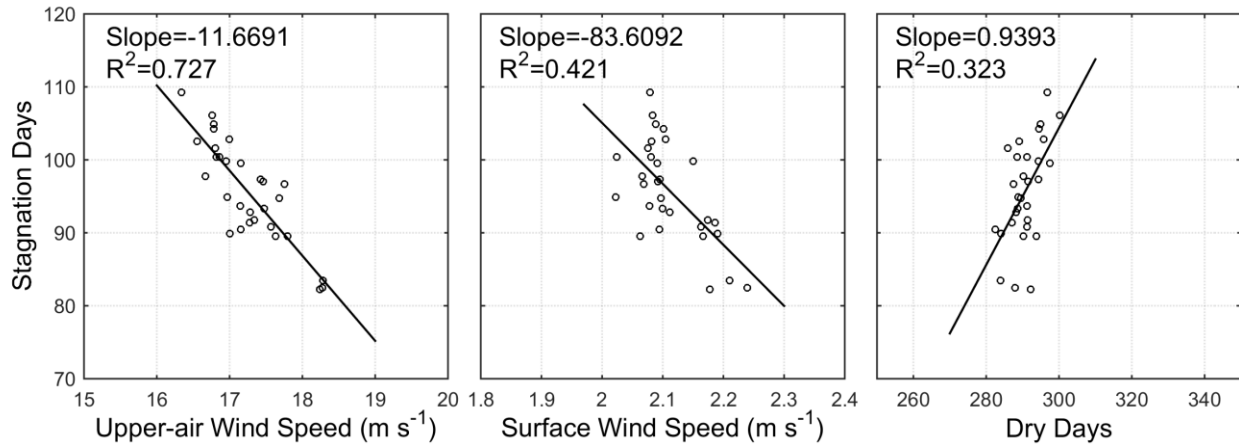
Figure 10. Same as Fig. 8, but for the trends of stagnant days. Linear regression coefficients between national averaged stagnant days in 30-year period and each corresponding component are shown.